Available online at www.sciencedirect.com
SCIENCE DIRECT®
European Polymer Journal 41 (2005) 231–237
EUROPEAN POLYMER JOURNAL
www.elsevier.com/locate/europolj

Cationic polymerization and physicochemical properties of a biobased epoxy resin initiated by thermally latent catalysts

Soo-Jin Park [a,*], Fan-Long Jin [a], Jae-Rock Lee [a], Jae-Sup Shin [b]

[a] *Advanced Materials Division, Korea Research Institute of Chemical Technology, P.O. Box 107, Yusong, Daejeon 305-600, South Korea*
[b] *Department of Chemistry, Chungbuk National University, Chongju 361-763, South Korea*

Received 30 July 2004; received in revised form 18 September 2004; accepted 20 September 2004
Available online 18 November 2004

Abstract

The cationic polymerization and physicochemical properties of a biobased epoxy resin, epoxidized castor oil (ECO), initiated by *N*-benzylpyrazinium hexafluoroantimonate (BPH) and *N*-benzylquinoxalinium hexafluoroantimonate (BQH) as thermally latent catalysts were studied. As a result, BPH and BQH show an activity at different temperatures in the present systems. The cured ECO/BPH system showed a higher glass transition temperature, a lower coefficient of thermal expansion, and higher thermal stability factors than those of the ECO/BQH system. On the other hand, the mechanical properties of the ECO/BQH system were higher than those of the ECO/BPH system. These have been attributed to the differences in crosslinking level of cured resins, which were induced by the different activity of the latent catalysts.

Keywords: Castor oil; Epoxy resin; Cationic polymerization; Thermal properties; Mechanical properties

1. Introduction

Replacement of petroleum-derivated raw materials with vegetable oil-based polymeric materials is important in the social and environmental viewpoints [1–4]. Vegetable oil from plant sources is readily regenerated via photosynthesis. Recently, a variety of vegetable oil has been developed with knowledge of their physical and chemical properties obtained through the application of scientific research and development [5,6]. Among them, castor oil represents a promising raw material based on its low toxicity and its availability as a renewable agricultural resource [7].

Several families of castor oil-based polymers are synthesized and investigated with respect to their physicochemical properties, such as thermal stabilities, flame retardancy, and mechanical properties. The castor oil or brominated castor oil used as reinforcing agent is added to epoxy resins and good toughness and flame retardancy of cured epoxy resins are obtained [8,9]. And the synthesis and properties of castor oil-based polyurethane hybrid materials has been reported [10]. Recently, the synthesis and thermal properties of epoxidized vegetable oil initiated by a thermally latent catalyst are also studied [11].

Latent catalysts are inert under normal conditions, i.e., at an ambient temperature and light, but they show activity by only certain external stimulation, such as

* Corresponding author. Tel.: +82 42 860 7234; fax: +82 42 861 4151.
E-mail address: psjin@krict.re.kr (S.-J. Park).

0014-3057/$ - see front matter © 2004 Elsevier Ltd. All rights reserved.
doi:10.1016/j.eurpolymj.2004.09.011

heating or photoirradiation. Latent catalysts are widely used on the synthesis of various polymeric materials, such as thermosetting resins, adhesives, paintings, inks, and photoresists [12]. In recent years, the cationic polymerization of thermosetting resins has been investigated intensively using various thermally latent cationic catalysts. Several classes of cationic catalysts, such as iodonium, ammonium, pyridinium, and sulfonium salts, have been developed as thermally latent and photolatent initiators for the polymerization of thermosetting resins [13–16]. Development of efficient latent catalysts is desirable for the enhancement of both storage stability and handling of thermosetting resins.

N-benzylpyrazinium and *N*-benzylquinolinium salts have been shown to be excellent latent initiators for epoxy resins. They dissolve readily in epoxy resins and exhibit a longer pot life than the more commonly used BF_3-4-methoxyaniline complex [17,18].

As previously mentioned, although many studies of epoxy/castor oil-based polymer blends have been described, but there little work has been reported on the cationic polymerization, thermal stabilities, and mechanical properties of epoxidized castor oil (ECO) initiated by cationic latent catalysts [8,9].

In this work, we present new data on the cationic polymerization and physicochemical properties of a biobased epoxy resin, ECO, initiated by *N*-benzylpyrazinium hexafluoroantimonate (BPH) and *N*-benzylquinoxalinium hexafluoroantimonate (BQH). The characterization of the properties was performed by differential scanning calorimetry (DSC), dynamic mechanical analysis (DMA), thermal mechanical analysis (TMA), thermogravimetric analysis (TGA), and an universal test machine (UTM).

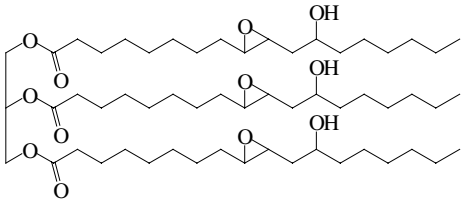

Epoxidized castor oil (ECO)

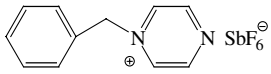

N-benzylpyrazinium hexafluoroantimonate (BPH)

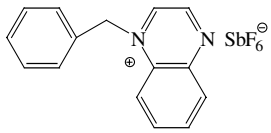

N-benzylquinoxalinium hexafluoroantimonate (BQH)

Fig. 1. Chemical structure of the materials used.

2. Experimental

2.1. Materials

ECO used in this study was synthesized by reaction of castor oil with glacial acetic acid and hydrogen peroxide using Amberite IR-120 as a catalyst in our lab scale [11,19]. BPH and BQH as cationic latent catalysts were prepared from previous work [18,20]. The chemical structures of ECO, BPH, and BQH are shown in Fig. 1.

2.2. Synthesis of epoxidized castor oil

Castor oil (91.8 g, 0.14 mol), glacial acetic acid (21.0 g, 0.35 mol), Amberlite (23 g), and toluene (40 g) were added to a 500 ml four-neck round-bottom flask equipped with a mechanical stirrer, thermometer sensor, and reflux condenser. The temperature was maintained at 55 °C. To this solution, 30% H_2O_2 (56.7 g, 0.5 mol) was added with stirring. The reaction was run at 55 °C for 7 h. The solution was then filtered and washed with a saturated solution of $NaCO_3$, distilled water, and then dried with anhydrous sodium sulfate. Finally, the toluene was removed by distillation under vacuum to give epoxidized castor oil, which was further dried under vacuum at 80 °C for 2 h: yield 84%.

FT-IR (cm^{-1}): 3009 (C=C), 843 (epoxide group).
^{1}H NMR ($CDCl_3$), δ (ppm): 5.3 (2H, C=C), 2.9–3.1 (2H, epoxide group).
^{13}C NMR ($CDCl_3$), δ (ppm): 129.7–130.2 (C=C), 54.0, 54.3 (epoxide group).

2.3. Sample preparation

One wt% catalyst (BPH or BQH) was dissolved in acetone and then was mixed with ECO at the ambient temperature. The mixture was fully stirred by a mechanical stirrer and then degassed in a vacuum oven before a DSC test. The preparation of the specimens for thermal and mechanical tests was as follows: The formulated mixtures were poured into the mold and cured first at 110 °C for 1 h, then at 140 °C for 2 h, and finally post cured at 160 °C for 1 h in a convection oven.

2.4. Characterization and measurements

IR spectrum was examined with a Bio-Rad Co. digilab FTS-165 spectrometer using KBr pellets. ^{1}H NMR

and ^{13}C NMR spectra were obtained from a BRUKER Co. DRX300 spectrometer operation at 300 MHz in chloroform-d.

The polymerization behaviors of ECO were performed at a heating rate of 10 °C/min in the range of 30–300 °C under nitrogen atmosphere with a dynamic differential scanning calorimeter (Perkin Elmer, DSC6). The latent initiation properties of the catalysts were evaluated by the measurement of the conversion as a function of the curing temperature with the isothermal DSC. The fraction conversion was obtained by integration of the areas under the curve in isothermal DSC thermograms.

Dynamic mechanical analysis (DMA) was performed using a dynamic mechanical analyzer (RDS-II, Rhemetrics Co.) at a frequency of 1 Hz and the temperature range from −50 to 150 °C at a scan rate of 5 °C/min. The sample size was approximately $3 \times 12 \times 60\,mm^3$.

The glass transition temperature of cured ECO samples was determined by thermal mechanical analysis (TMA). TMA was carried out by a RDS-II (Rhemetrics Co.) at a heating rate of 5 °C/min under a nitrogen atmosphere. The approximate sample size was $5 \times 10 \times 10\,mm^3$.

Thermogravimetric analyses were performed with a du Pont TGA-2950 analyzer to investigate the thermal degradation from 30 to 850 °C at a heating rate of 10 °C/min in the nitrogen atmosphere.

The tearing energy was characterized by trouser beam tests. The sample size was $2 \times 25 \times 75\,mm^3$ and the crosshead displacement rate was 1 mm/min. The tensile properties of the specimens were measured on a universal tester (Instron Model 1125 mechanical tester) at ambient temperature according to ASTM D 638-95. All mechanical property values were obtained by averaging the five experimental values.

3. Results and discussion

3.1. Polymerization of ECO using BPH and BQH

Fig. 2 shows the dynamic DSC curves for the polymerization of ECO initiated by BPH and BQH at a heating rate of 10 °C/min. From the DSC thermograms, the obtained peak maximum temperature and enthalpy of the ECO/BPH and ECO/BQH systems are 158 °C, 173 J/g and 142 °C, 154 J/g, respectively. The results indicate that the polymerization of the ECO/BPH system is performed at higher temperature than that of the ECO/BQH system.

The cationic polymerization of ECO was carried out in the presence of 1 wt% thermally latent catalysts, BPH and BQH, at 50–120 °C for 2 h [10,21]. The catalysts are completely soluble in epoxy resins at ambient temperature, and the polymerization is performed homogeneously. The proton acid is formed by the thermal decomposition of BPH and BQH, and catalyzes the cationic polymerization of the epoxides. Fig. 3 shows the conversion of the ECO/BPH and ECO/BQH systems as a function of temperature. The polymerization of the ECO/BPH and ECO/BQH systems is initiated above 60 °C for BPH and above 50 °C for BQH, whereas no polymerization proceeded below 50 °C. The bond between a nitrogen atom and a carbon atom of BPH and BQH is thermally cleaved to generate benzyl cationic initiating species, as shown in Scheme 1. The N—C bond of BQH is easily cleaved than that of BPH, which due to the larger resonance delocalization effect by the phenyl group on BQH [22]. And both of the polymerizations occur rapidly above these temperatures. Therefore, BPH and BQH are excellent thermally latent initiator that functions in the absence of co-initiator and shows

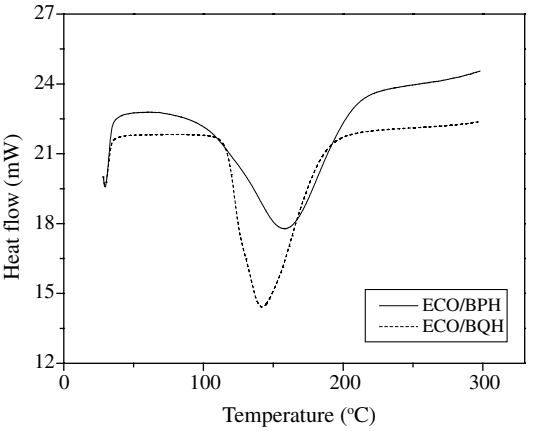

Fig. 2. Dynamic DSC thermograms of the ECO/BPH and ECO/BQH systems.

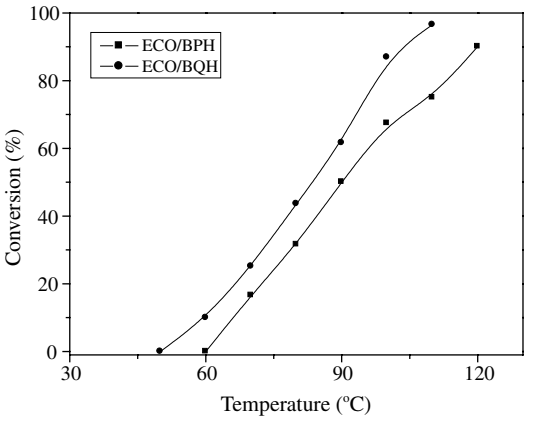

Fig. 3. Conversion of the ECO/BPH and ECO/BQH systems as a function of temperature.

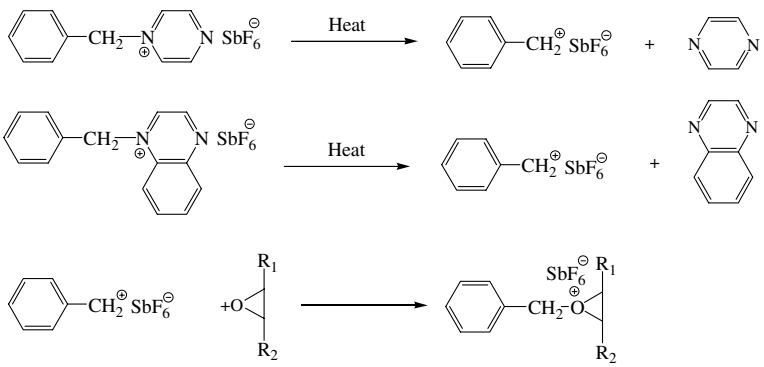

Scheme 1. Initiation step in the polymerization mechanisms of epoxides initiated by BPH and BQH.

an activity at different temperatures in the present systems [11].

3.2. Dynamic mechanical analysis

The storage modulus in the plateau over the α-relaxation is related to the crosslinking density of the cured resins. The tan δ and storage modulus of cured ECO/BPH and ECO/BQH samples were measured a wide temperature range −50 to 150 °C at a heating rate of 5 °C/min, and are shown in Figs. 4 and 5. From these figures, the ECO/BPH system showed a relatively higher α-relaxation temperature and storage modulus than those of the ECO/BQH system.

The crosslinking density (ρ) of cured samples is calculated from the equilibrium storage modulus in the rubber region over the α-relaxation temperature according to the rubber elasticity theory [23], as follows:

$$\rho = \frac{G'}{\phi RT}, \tag{1}$$

where T_α is the α-relaxation temperature, G' the storage modulus at $T_\alpha + 30$ °C, ϕ the front factor, R the gas constant, and T the absolute temperature at $T_\alpha + 30$ °C.

The obtained T_α, G', and ρ are summarized in Table 1. The results indicate that the crosslinking densities

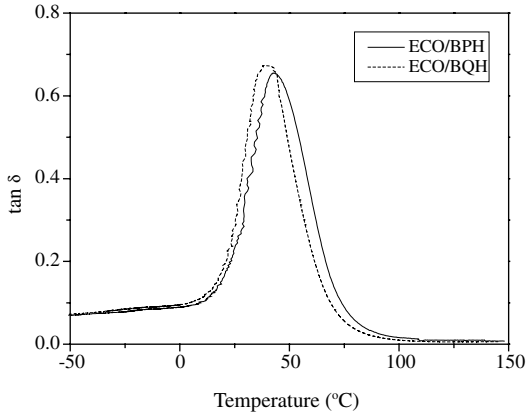

Fig. 4. tan δ of the ECO/BPH and ECO/BQH systems as a function of temperature.

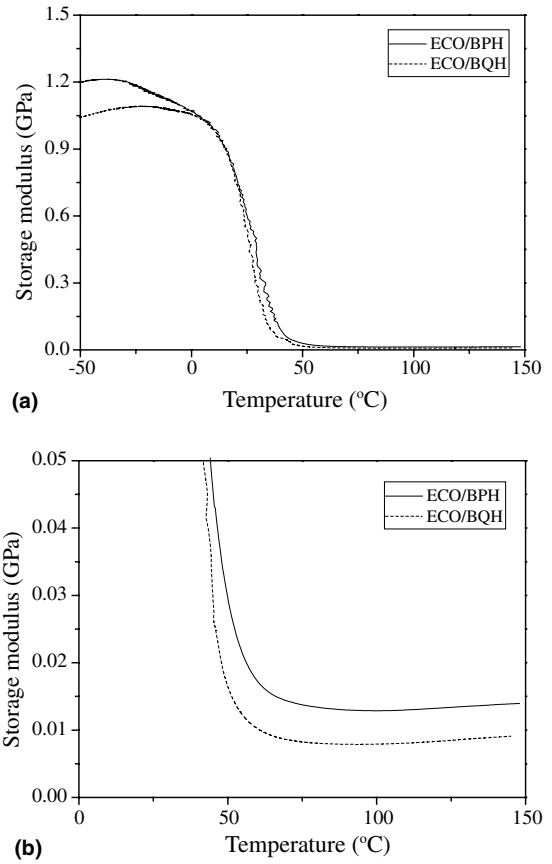

Fig. 5. Storage modulus of the ECO/BPH and ECO/BQH systems at two different storage modulus ranges: (a) 0–1.5 GPa; (b) 0–0.05 GPa.

Table 1
Dynamic mechanical analysis of cured ECO/BPH and ECO/BQH systems

System	T_α (°C)	Storage modulus (GPa)		ρ (10^{-3} mol/cm^3)
		Glassy region[a]	Rubbery region[b]	
ECO/BPH	43	0.36	0.014	1.01
ECO/BQH	39	0.25	0.009	0.84

[a] Storage modulus at 30 °C.
[b] Storage modulus at T_α + 30 °C.

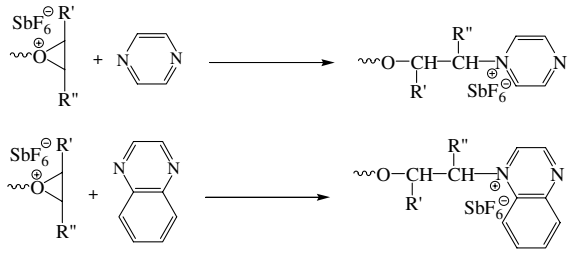

Scheme 2. Termination step in the polymerization mechanisms of epoxides initiated by BPH and BQH.

of cured ECO/BPH and ECO/BQH samples are 1.01×10^{-3} and 0.84×10^{-3} mol/cm^3, respectively. Differences in crosslinking density of cured resins can be attributed to the different reactivity of latent catalysts in the termination step of the polymerization. In Scheme 2, when the epoxy concentration decreased, the pyrazine or benzopyrazine released from the salts could attack predominantly propagation species to terminate the polymerization. The lower crosslinking density can be due to the higher terminating ability of benzopyrazine induced by decreased electron density of nitrogen by resonance delocalization effect of the phenyl group in the ECO/BQH system [24].

3.3. Thermal mechanical analysis

The glass transition temperature (T_g) and coefficient of thermal expansion (CTE) of the ECO/BPH and the ECO/BQH systems were studied with TMA at a heating rate of 5 °C/min in a nitrogen atmosphere. The T_g value was taken at the intercept between the regression line and inflectional tangent line from the curve of the linear CTE as a function of temperature. The obtained T_g and CTE of the systems are presented in Table 2. The ECO/BPH system shows a higher T_g value and a lower CTE in both the glassy and rubbery regions than those of the ECO/BQH system. This result may be caused by the crosslinking density of the ECO/BPH system being higher than that of the ECO/BQH system [25].

Table 2
Thermal mechanical analysis of cured ECO/BPH and ECO/BQH systems

System	T_g (°C)	CTE ($\times 10^{-5}$, °C^{-1})	
		Glassy region	Rubbery region
ECO/BPH	38 ± 1	10.8 ± 0.2	20.5 ± 0.3
ECO/BQH	30 ± 1	11.8 ± 0.3	21.1 ± 0.3

3.4. Thermal stabilities

The thermal degradation behaviors of the ECO/BPH and ECO/BQH systems were studied with TGA at a heating rate of 10 °C/min in the nitrogen atmosphere and the TGA thermograms are shown in Fig. 6. The ECO/BPH and ECO/BQH systems present similar degradation behaviors. It is found that the degradation of cured ECO is a two-stage process. A relatively short stage with a 5% weight loss happened at about 340 °C, which is attributed to the breaking of impurity traces apart from the cured ECO network. Above 390 °C, the main process is a much higher thermal-resistant stage, and this is caused by thermal degradation of cured ECO network [19].

Thermal stability factors, including initial decomposed temperature (IDT; 5% weight loss), temperatures of the maximum rate of degradation (T_{max}), and the decomposition activation energy (E_d), can be determined from TGA thermograms [26].

The decomposition activation energy (E_d) of the systems is calculated from TGA curves by the integral method of Coats and Redfern's equation, as follows [27]:

$$\ln \frac{\alpha}{T^2} = \ln \frac{AR}{\beta E_d}\left(\frac{1-2RT}{E_d}\right) - \frac{E_d}{RT}, \quad (2)$$

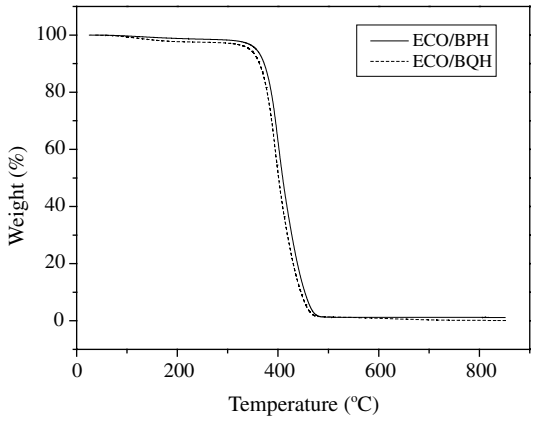

Fig. 6. TGA thermograms of the ECO/BPH and ECO/BQH systems.

Table 3
Thermal stability factors of cured ECO/BPH and ECO/BQH systems

System	IDT (°C)	T_{max} (°C)	E_d (kJ/mol)
ECO/BPH	351	395	128
ECO/BQH	344	394	119

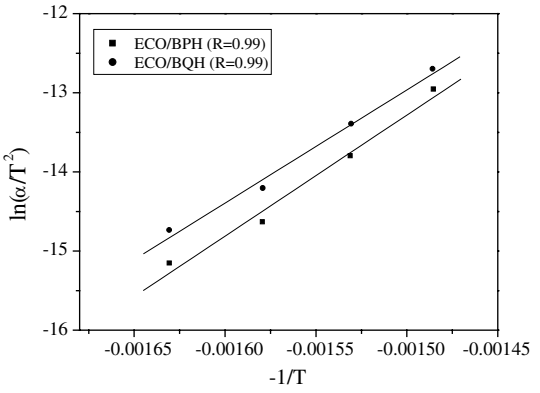

Fig. 7. Plots of $\ln(\alpha/T^2)$ vs. $(-1/T)$ for the ECO/BPH and ECO/BQH systems.

where α is the decomposed fraction, T the temperature of maximum rate of degradation, A the preexponential factor, β the heating rate, and R the gas constant.

The calculated IDT and T_{max} are listed in Table 3. The plots of $\ln(\alpha/T^2)$ vs. $(-1/T)$ are shown in Fig. 7. The E_d of the systems was calculated from the slope of the straight lines using the Eq. (2) and presented in Table 3. As a result, the IDT and E_d values of the ECO/BPH system are higher than those of the ECO/BQH system. This has been attributed to the network crosslinking density of the ECO/BPH system is higher than that of the ECO/BQH, as mentioned in the TMA result [25].

3.5. Mechanical properties

The mechanical properties of the ECO/BPH and ECO/BQH systems are determined in terms of the tensile properties and tearing energy (G_{IIIC}), respectively. The tearing energies are calculated using the following equation:

$$G_{IIIC} = \frac{2F}{t}, \quad (3)$$

where F is the applied force and t is the width of the tear path.

The results of the tearing energy and tensile properties are presented in Table 4. The tearing energy and tensile strength of the ECO/BQH system are much higher than those of the ECO/BPH. The elongation at the break of the ECO/BQH is also higher than that of the ECO/BPH. Differences in mechanical properties between two systems can be attributed to differences in crosslinking level of cured resins, which are induced by the different activity of latent catalysts.

Table 4
Mechanical properties of cured ECO/BPH and ECO/BQH systems

System	G_{IIIC} (J/m^2)	Tensile strength (MPa)	Elongation at break (%)
ECO/BPH	315 ± 12	1.7 ± 0.1	23 ± 1
ECO/BQH	425 ± 17	2.5 ± 0.1	26 ± 1

4. Conclusion

In this work, the effects of cationic latent catalysts on the cationic polymerization, thermal stabilities, and mechanical properties of ECO were investigated. As a result, BPH and BQH showed activity at 60 and 50 °C, respectively. The glass transition temperature, coefficient of thermal expansion, and thermal stability factors of the ECO/BPH system were higher than those of the ECO/BQH system. On the contrary, the mechanical properties of the ECO/BQH system were higher than those of the ECO/BPH system. These could be attributed to the crosslinking density of the ECO/BPH system being higher than that of the ECO/BQH system.

References

[1] Uyama H, Kuwabara M, Tsujimoto T, Kobayashi S. Biomacromolecules 2003;4:211–5.
[2] Tsujimoto T, Uyama H, Kobayashi S. Macromolecules 2004;37:1777–82.
[3] Ahmad S, Haque MM, Ashraf SM, Ahmad S. Eur Polym J 2004;40:2097–104.
[4] Chakrapani H, Liu C, Widenhoefer RA. Org Lett 2003;5:157–9.
[5] Kaplan DL. Biopolymers from renewable resources. Berlin: Springer; 1998. p. 1–3.
[6] Tan CP, Che Man YB. Photochem Anal 2002;13:129–41.
[7] Srivastava A, Singh P. Polym Adv Technol 2002;13:1055–66.
[8] Raymond MP, Bui VT. J Appl Polym Sci 1998;70:1649–59.
[9] Xiao WD, He PX, He BQ. J Appl Polym Sci 2002;86:2530–4.
[10] Hu YS, Tao Y, Hu CP. Biomacromolecules 2001;2:80–4.
[11] Park SJ, Jin FL, Lee JR. Macromol Rapid Commun 2004;25:724–7.
[12] Kobayashi M, Sanda F, Endo T. Macromolecules 2000;33:5384–7.
[13] Crivello JV. J Polym Sci Polym Chem 1999;37:4241–54.
[14] Goh Y, Iijima T, Tomoi M. J Polym Sci Polym Chem 2002;40:2702–16.
[15] Park SJ, Kim HC. J Polym Sci Polym Phys 2001;39:121–8.

[16] Lee SD, Takata T, Endo T. Macromolecules 1996;29:3317–9.
[17] Morio K, Murase H, Tsuchiya H, Endo T. J Appl Polym Sci 1985;32:5727–32.
[18] Park SJ, Seo MK, Lee JR, Lee DR. J Polym Sci Polym Chem 2001;39:187–95.
[19] Park SJ, Jin FL, Lee JR. Macromol Chem Phys 2004;205:2045–54.
[20] Park SJ, Kim HC, Lee HL, Suh DH. Macromolecules 2001;34:7573–5.
[21] Takahashi E, Sanda F, Endo T. J Polym Sci Polym Chem 2002;40:1037–46.
[22] Toneri T, Sanda F, Endo T. Macromolecules 2001;34:1518–21.
[23] Iijima T, Yoshioka N, Tomoi M. Eur Polym J 1992;28:573–81.
[24] Kim MS, Lee KW, Endo T, Lee SB. Macromolecules 2004;37:5830–4.
[25] Xie MR, Wang ZG. Macromol Rapid Commun 2001;22:620–3.
[26] Doyle CD. Anal Chem 1961;33:77–9.
[27] Coats AW, Redferm JW. J Polym Sci Polym Lett 1965;3:917–20.